Contents lists available at ScienceDirect

Organic Geochemistry

journal homepage: www.elsevier.com/locate/orggeochem

Chemical and carbon isotopic dynamics of grass organic matter during litter decompositions: A litterbag experiment

Guoan Wang [a], Leilei Zhang [a], Xinyu Zhang [b], Yinghui Wang [b], Yunping Xu [b,c,∗]

[a] Department of Environmental Science and Technology, College of Resources and Environmental Sciences, China Agricultural University, Beijing 100193, China
[b] MOE Key Laboratory for Earth Surface Process, College of Urban and Environmental Sciences, Peking University, Beijing 100871, China
[c] Qingdao Collaborative Innovation Center of Marine Science and Technology, Qingdao 266003, China

ARTICLE INFO

ABSTRACT

A litterbag method was used for studying the variability in chemical and carbon isotopic compositions of four grasses during litter decomposition. After the 300 d degradation, > 90% of litter mass was lost for three C_4 species (*Setaria viridis*, *Eleusine indica*, *Amaranthus retroflexus*) and one C_3 species (*Erigeron speciosus*). The solid state ^{13}C NMR spectra showed that mean proportion of aromatic and alkyl carbon increased from *ca.* 10% to 15% and *ca.* 10% to 20%, respectively, whereas that of *O*-alkyl carbon substantially decreased from *ca.* 70% to 50%. The carbon preference index and average chain length of *n*-alkanes remained relatively constant, whereas the carbon isotopic compositions of long chain *n*-alkanes varied < 2‰. Our results demonstrate that the degradation of litters alone does not significantly change the *n*-alkane chemical and carbon isotopic proxies. Compared to open plant–soil systems, our litterbag experiments present much less variability in chemical and carbon isotopic compositions of *n*-alkanes. Based on these facts, we recommend a combined measurement of chemical and carbon isotopic properties in evaluation of carbon sources, dynamics and paleoenvironments.

1. Introduction

As an important source for soil and sediment organic matter, plants differ in carbon isotopic compositions due to different photosynthetic pathways and environmental conditions (Deines, 1980; O'Leary, 1981; Farquhar et al., 1989; Blagodatskaya et al., 2011; Wang et al., 2013a). The mean δ^{13}C of C_3 and C_4 plants is −27‰ and −13‰, respectively (O'Leary, 1981; Meyers, 1997). For C_3 plants alone, the $\delta^{13}C_{leaf}$ decreases with increasing rainfall by a coefficient of *ca.* −1.1‰/100 mm (Wang et al., 2008), whereas the $\delta^{13}C_{leaf}$ increases with temperature by a coefficient of *ca.* 0.104‰/°C (Wang et al., 2013a). Consequently, the carbon isotopic composition is a useful tracer for documenting organic carbon sources, dynamics and past vegetation changes (Boutton, 1996; Diefendorf et al., 2010; Kohn, 2010; Vandenbroucke et al., 2013). However, the decomposition process also affects δ^{13}C due to the selected degradation of individual constitutes and incorporation of ^{13}C enriched microbial biomass (Wedin et al., 1995; Feng, 2002). A number of studies have reported that ^{13}C enrichment occurred during decomposition such that the soil organic matter

tends to have higher δ^{13}C values than the vegetation (Boutton, 1996; Bird and Pousai, 1997; Wang et al., 2008).

Compared to bulk carbon isotope analysis, compound specific isotope analysis (CSIA) has an apparent advantage since this method measures individual biomarkers with specific sources and thereby reduces interferences from different constituents and source carbon (Hayes et al., 1990). Among various biomarker types, *n*-alkanes are the most commonly investigated molecules for CSIA because of their ubiquitous distributions in the environment, resistance to degradation and relatively easy analyses (Eglinton and Hamilton, 1967). Biogenic *n*-alkanes in the environment usually occur as a series of homologues with carbon numbers from 15–35 (Meyers, 1997). The long chain *n*-alkanes (C_{25}–C_{35}) with a strong odd/even predominance (OEP) are mainly derived from vascular plants, whereas the short chain *n*-alkanes (C_{15}–C_{20}) with much lower OEP are of a algal/microbial origin (Meyers, 1997). Given this fact, carbon preference index (CPI) and average chain length (ACL) have been proposed for estimating the sources of *n*-alkanes (Meyers, 1997; Zhang et al., 2006; Bush and McInerney, 2013), defined as:

$$CPI = \frac{1}{2}\left(\frac{C25+C27+C29+C31+C33}{C24+C26+C28+C30+C32} + \frac{C25+C27+C29+C31+C33}{C26+C28+C30+C32+C34}\right)$$

$$ACL = \frac{\sum_x \times C_x}{\sum C_x}$$

∗ Corresponding author at: MOE Key Laboratory for Earth Surface Process, College of Urban and Environmental Sciences, Peking University, Beijing 100871, China. Tel.: +86 10 62752019.

E-mail address: yunpingxu@pku.edu.cn (Y. Xu).

where C_x is the concentration of n-alkane with x carbon atoms.

Based on a 23 y litterbag experiment, Huang et al. (1997) concluded the absence of carbon isotopic fractionation of long chain n-alkanes during early diagenesis. That study, however, was conducted in anaerobic peat and may not represent the more widely distributed aerobic soil environments. Nguyen Tu et al. (2011) conducted a 4 yr litterbag experiment using the European beech leaves and the results showed that the $\delta^{13}C$ values of n-alkanes were nearly constant for unlabelled leaves, but substantially decreased for ^{13}C labelled leaves. These changing patterns were used as evidence for a microbial contribution to the long chain alkane pool of the decomposing leaves (Nguyen Tu et al., 2011). In contrast to the litterbag experiments, open plant–soil systems usually presented significant ^{13}C enrichments of long chain n-alkanes from raw leaves to soil (Nguyen Tu et al., 2004; Chikaraishi and Naraoka, 2006). The reason for large $\delta^{13}C$ shifts is not clear, but probably include diagenetic effects, variability in carbon isotopic compositions among different plants and external carbon inputs from soil microbes and fauna.

Besides $\delta^{13}C$, the n-alkane distribution pattern may be also sensitive for organic matter decomposition. From plants to soils, the proportion of mid-chain (C_{23} and C_{25}) n-alkanes increased (Almendros et al., 1996), whereas the OEP and CPI decreased (Huang et al., 1996; Jansen and Nierop, 2009; Buggle et al., 2010). Since these studies were conducted in the open soil systems, many factors responsible for the ACL, CPI and OEP shifts, such as different degradation rates of n-alkane homologues, contributions from different vegetation with different n-alkane compositions and external n-alkane interferences from soil microbes or pre-aged organic matter, can co-exist (Huang et al., 1996; Marseille et al., 1999; Chikaraishi and Naraoka, 2006; Buggle et al., 2010). In contrast, the litterbag experiment is performed in a relatively closed system, allowing observations of known amounts of initial litters of known species/tissues at the known degradation time, thereby greatly reducing uncertainties that exist in the open plant–soil systems (Wider and Lang, 1982).

Here we used the litterbag method to trace chemical and carbon isotopic dynamics of four grass species during litter decomposition. These grasses include three C_4 plants (Setaria viridis, Eleusine indica, Amaranthus retroflexus) and one C_3 plant (Erigeron speciosus). The reasons we chose these C_3 and C_4 grass species are that: (1) most of previous studies about litter decompositions focused on tree leaves, whereas grasses have been rarely investigated (Nguyen Tu et al., 2004, 2011; Chikaraishi and Naraoka, 2006); (2) the grasses used in our study are common species in China and even in most continents and therefore are good models for the decomposition of grass litters; and (3) the appearance of C_4 vegetation on the earth is closely correlated with climate and atmosphere and thus the relative abundance of C_3/C_4 plants in the environment is a useful tracer for past climate (Ehleringer et al., 1991; Collatz et al., 1998). By analyzing biomarkers, solid state ^{13}C NMR and carbon isotopic compositions of litters in the 300 d decomposition experiments, we attempted to (1) determine the magnitude and direction of carbon isotopic shifts of individual n-alkanes; (2) evaluate the degradation effect on n-alkane indicators (e.g., CPI, ACL); and (3) assess relative importance of each factor such as different $\delta^{13}C$ values among different plants, external carbon inputs from soil fauna and microbes and kinetic isotopic fractionation responsible for the $\delta^{13}C$ alteration during litter decomposition processes.

2. Material and methods

2.1. Litterbag method

The study area is located in the western suburbs of Beijing. The local climate is dominated by temperate continental monsoon with an annual mean temperature of 13 °C and annual precipitation of 480 mm. Four grass species including three C_4 plants (S. viridis, E. indica, A. retroflexus) and one C_3 plant (E. speciosus) were used for the litterbag experiment. Brown grasses were collected and rinsed carefully with distilled water and dried at 40 °C. Nylon bags (120 mm × 150 mm; 0.1 mm mesh size) each containing 5 g of litter were placed on surface soils in the Shangzhuang Experimental Station (China Agricultural University, Beijing) and covered by about 5 cm of soil. This agricultural station has the total area of 70 hm² and is cultivated with a wheat/maize rotation. The soil is dominated by silt (55.2 ± 7.6%; mean ± SD), followed by sand (32.4 ± 10.1%) and clay (12.5 ± 9.5) (Hu et al., 2006). The pH of soil is 8.13 ± 0.17, while the concentration of soil organic matter is 10.9 ± 4.8 g/kg (Hu et al., 2006). The litterbag experiment was conducted from December 2011 to October 2012, and the samples were harvested every 30 days (3 replicates). The soil particles were removed as carefully as possible. The remaining litter was dried at 40 °C until constant weight was reached. After that, the litters were ground into powder (< 100 μm). The replicate samples were analyzed individually for mass loss, biomarkers and carbon isotopic composition. After that, the remaining replicate samples were homogenized for the analyses by solid state ^{13}C NMR.

The decomposition rate was calculated according to a negative exponential curve, expressed as:

$$M_t = M_0 e^{-kt}$$

M_0 is the initial litter mass; M_t is the mass remaining at the decomposition time t; k is the decay rate constant.

2.2. ^{13}C NMR spectroscopy

Solid state ^{13}C NMR measurements were performed on a Bruker AV-300 spectrometer equipped with a 4 mm wide-bore magic angle spinning (MAS) probe. The NMR was operated at a frequency of 75.5 MHz. The powdered samples were packed in a 4 mm zirconia rotor with Kel-F caps and spun at a rate of 4 kHz. A standard cross-polarization pulse sequence was used, with single contact times of 2 ms and a recycle delay of 5 s. The number of scans was 500–600. The ^{13}C NMR spectra were divided into four regions according to chemical shift: alkyl C (0–50 ppm) mainly including cutins, suberins and wax lipids; O-alkyl C (50–110 ppm) derived from carbohydrates, celluloses and hemicelluloses; aromatic C (110–160 ppm) from polyphenols, lignins and tannins; and carbonyl C (160–220 ppm) from carboxylic acids, amides and organic acids (Kögel-Knabner, 1997). The proportion of each type carbon was calculated by the integration of the spectral regions.

2.3. Biomarker analysis

After addition of 5.6 μg squalane (internal standard), 0.5 g litter samples were ultrasonically extracted with 10 ml dichloromethane:methanol (3:1 v:v) for 15 min (3×). The combined extracts were rotary evaporated to near dryness and further completely dried under a mild nitrogen stream. After re-dissolved in 1.0 ml hexane, the extract was separated into an apolar fraction (10 ml hexane:dichloromethane; 9:1 v:v) and a polar fraction (10 ml dichloromethane:methanol; 1:1 v:v) over a silica gel column chromatograph. The apolar fraction containing n-alkanes were blown to dryness under a mild nitrogen stream and re-dissolved in 1.0 ml hexane before instrumental analysis.

The compounds were identified by a gas chromatography–mass spectrometer (GC–MS) composed of an Agilent 7890A GC and an Agilent 5975C Series mass selective detector (MSD). A DB5-MS column (30 m × 0.25 mm i.d., film thickness 0.25 μm, Agilent) was used with high purity helium (> 99.999%) as the carrier gas. The

MSD was operated in the electron ionization mode at 70 eV with a scan range of 50–650 Da. Data were acquired and processed with the Chemstation software. The GC oven temperature increased from 60–300 °C at a rate of 6 °C/min and held at 300 °C for 20 min.

An Agilent 7890A GC equipped with a flame ionization detector (FID) was used for the quantification of biomarkers. The column was an HP 5 capillary column (Agilent HP-5, 30 m; 0.32 mm i.d.; 0.25 μm film thickness). The injector temperature was 300 °C. A 1 μl of sample was injected in splitless mode. Helium (99.999% purity) was carrier gas. The GC oven temperature increased from 60–300 °C at a rate of 6 °C/min and held at 300 °C for 20 min. External calibrations were conducted which showed the relative response factor (RRF) of long chain n-alkanes to squalane was 0.94–0.96. Therefore, a RRF of 1.0 was used to determine the amount of n-alkanes by comparison of respective peak areas to squalane.

2.4. Compound specific carbon isotope analysis (CSIA)

A detailed method for the CSIA of n-alkanes has been described by Huang et al. (2012). Briefly, a gas chromatograph-combustion-isotope ratio mass spectrometer (GC-C-IRMS) composed of a Finnigan Trace GC and a Finnigan Delta XP isotope ratio mass spectrometer was used for the $\delta^{13}C$ measurement. Samples were injected in splitless mode (1 μl) at 290 °C. Separation was achieved on a DB-5 MS column (60 m × 0.25 mm i.d., film thickness 0.25 μm). The oven temperature program of GC-C-IRMS was same as that of GC-FID. Only those $\delta^{13}C$ data with reproducibility better than ± 0.5‰ (standard deviation) were used. The carbon isotope composition was reported in the δ notation (‰) relative to the Vienna Peedee Belemnite (V-PDB) standard.

2.5. Statistical analysis

The program package SPSS 18.0 (Illinois, USA) was used for the statistical analyses. One-way ANOVA analysis was conducted to examine the differences in mass loss, chemical composition and the $\delta^{13}C$ values at different decomposition time. All analyses were performed with a significance level of $P < 0.05$.

3. Results

3.1. Mass loss patterns

Throughout the decomposition, the four grass species showed similar patterns of mass loss ($P = 1.00$; Fig. 1). At the termination of the litterbag experiment, > 90% of the initial mass was lost for all grass species (Fig. 1). Two distinct phases were observed with a slow degradation rate from December to April (0.2%/d) and a rapid degradation rate from April to October (3–6%/d).

3.2. Solid state ^{13}C NMR

Due to limited availability of samples, two species, S. viridis and E. indica, were selected for cross-polarization magic angle spinning (CPMAS) solid state ^{13}C nuclear magnetic resonance (NMR). Chemical compositions indicated by the NMR spectra continuously changed with degradation (Fig. 2). In undegraded litters, O-alkyl carbon accounted for 73% in S. viridis and 72% in E. indica. After 300 d decompositions, the proportion of O-alkyl carbon decreased to 58% in S. viridis and 50% in E. indica. In contrast, the relative abundance of alkyl and aromatic carbon substantially increased from ca. 10–15% in S. viridis and ca. 10–20% in E. indica. Carbonyl carbon remained relatively constant for S. viridis (6–8%), but increased for E. indica (7.6–13%). The alkyl/O-alkyl carbon ratio, an indicator for degree of organic matter degradation (Baldock et al.,
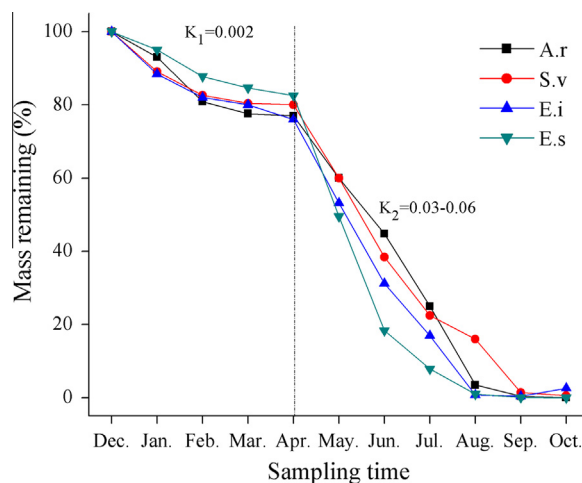

Fig. 1. Mass remaining (%) of grass litters in the litterbag experiments.

1995), substantially increased from 0.14 to 0.26 for S. viridis and 0.14 to 0.30 for E. indica.

3.3. Bulk and molecular compositions during decomposition

The concentration of carbon (C%) and nitrogen (N%), atomic C/N ratio and $\delta^{13}C$ in litters are shown in Table 1. With decomposition, C% decreased from 43.0% to 39.8% in A. retroflexus and 38.9% to 36.2% in E. indica, but slightly increased from 37.9% to 38.3% in S. viridis. In contrast, N% increased by 0.4–1.0% in all measured litters. The atomic C/N ratio substantially decreased in A. retroflexus (22.4–17.0), S. viridis (27.6–16.6) and E. indica (26.2–14.2).

In undegraded litters, the n-alkane homologues had carbon numbers from 23–35 and concentrations of 95–944 μg/g. The n-alkanes showed different degradation patterns among different grass species. Their concentrations of A. retroflexus and E. indica generally decreased with the litter decomposition and were only 52.7% and 68.0% after 210 d of decomposition (Table 2). In contrast, the n-alkane concentrations of S. viridis and E. speciosus generally increased with litter decomposition and were 130% and 33.6% higher after 180 d of decomposition than initial concentrations (Table 2). These differences suggest that the n-alkane degradation in litters is a complex process, which is dependent on not only chemical properties, but also plant species. In contrast to apparent changes of n-alkane abundance, the distribution pattern of n-alkanes did not change substantially. Throughout the 300 d litterbag experiment, the n-alkanes of the four grass species were constantly dominated by C_{31} and C_{29}, whereas the ACL fell in narrow ranges of 28.5–29.1 in S. viridis, 29.8–31.6 in E. indica, 29.3–31.0 in A. retroflexus and 30.6–31.6 in E. speciosus. Except for A. retroflexus, the other three species (S. viridis, E. indica and E. speciosus) showed a slight increasing trend for ACL after 120 d of decomposition (Fig. 3), reflecting preferential degradation of short chain n-alkanes relative to their long chain counterparts. A. retroflexus has remarkably lower CPI values (1.4–3.7) than other grass species (Fig. 3). The reason for this difference remained elusive, but A. retroflexus is unique in containing abundant iso- and anteiso-alkanes with the carbon number of 29–32. For E. indica, S. viridis and E. speciosus, their CPI values of n-alkanes stayed at high levels (7.7–10.8) throughout the litterbag experiment, although a slight decrease was observed after 150 d of decomposition (Fig. 3).

3.4. Variability in $\delta^{13}C$ of bulk organic matter and specific compounds

From the start to 180 d of decomposition, the $\delta^{13}C$ value of grass litters varied from −15.1 ± 0.7‰ to −15.3 ± 0.7‰ for A. retroflexus,

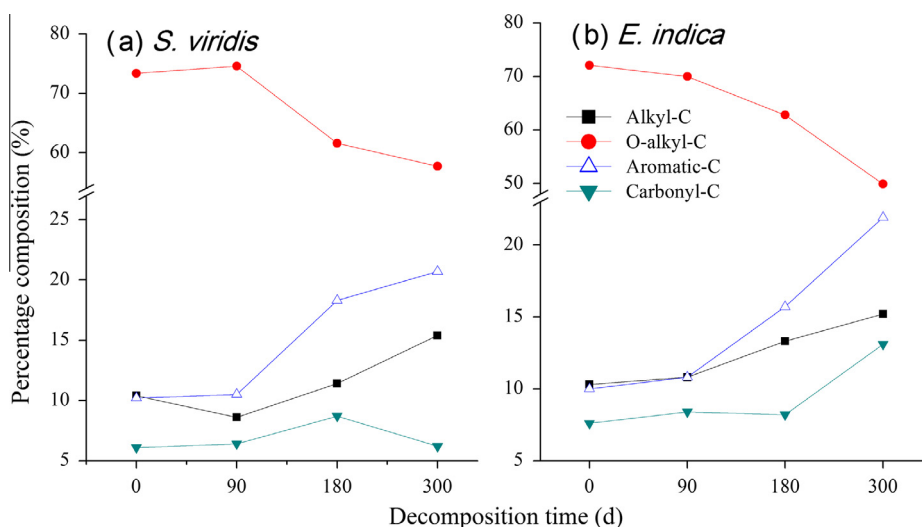**Fig. 2.** Relative ^{13}C NMR intensities of different type C in grass litters of *S. Viridis* and *E. indica*.

−14.5 ± 0.8‰ to −14.8 ± 0.2‰ for *S. viridis*, −15.9 ± 0.2‰ to −16.3 ± 0.3‰ for *E. indica*, and −33.7 ± 0.3‰ to −34.2 ± 0.2‰ for *E. speciosus*. Statistical analyses showed no significant difference in δ^{13}C between initial and degraded litters (P = 0.19–0.95). The minor decrease of the δ^{13}C value with litter decomposition likely reflects selected preservation of ^{13}C depleted lignin and alkyl constitutes, which is consistent with our NMR data as well as previous findings (Wedin et al., 1995; Feng, 2002).

Due to limited availability of samples, only *S. viridis* and *E. indica* were used for CSIA. The δ^{13}C signal of long chain n-alkanes (C$_{29}$, C$_{31}$ and C$_{33}$) varied from −23.3‰ to −25.4‰ for *S. viridis* and −24.0‰ to −25.7‰ for *E. indica* (Fig. 4), presenting typical values for lipids in C$_4$ plants (Collister et al., 1994). The 9–11‰ depletion in ^{13}C of n-alkanes compared to the bulk litters fell in the range of previous reports (O'Leary, 1981; Farquhar et al., 1989), reflecting an kinetic isotopic effect during lipid biosynthesis (Rieley et al., 1993; Chikaraishi and Naraoka, 2006). With the litter decomposition, the δ^{13}C values of C$_{29}$ to C$_{33}$ n-alkanes show an apparent positive shift in a magnitude of < 2‰ for *S. viridis* and *E. indica* (Fig. 4). However, the statistical analyses revealed no significant difference between initial and degraded litters (P = 0.18–0.62) due to relatively large standard error of δ^{13}C for long chain n-alkanes.

4. Discussion

4.1. Influence of climate on mass loss patterns of grass litters

The decomposition patterns in our study (Fig. 1) are remarkably different from previous observations that a rapid decay phase (loss of acid soluble carbohydrates) was usually followed by a slow

Table 2
Relative abundance of n-alkanes of grass litters throughout the litterbag experiments.

Decomposition time (days)	A. retroflexus	S. viridis	E. indica	E. speciosus
0	100.0	100.0	100.0	100.0
30	76.1	223.0	111.9	173.8
60	84.9	130.6	93.2	141.4
90	85.8	171.1	93.8	75.8
120	72.4	165.1	108.7	94.1
150	110.4	155.0	67.5	114.2
180	78.2	223.0	60.6	133.6
210	52.7	137.6	68.0	–

decay phase (loss of recalcitrant components such as lignin) (Melillo et al., 1989; Cortez, 1998; Prescott et al., 2000; Ono et al., 2009; Wang et al., 2013b). It is well known that climate and litter chemistry are the most important factors for the litter degradation (Murphy et al., 1998; Li et al., 2011; Wang et al., 2013b). Considering similar chemical compositions among the investigated grass species (see NMR data in Section 3.2), we only consider the climatic effect on litter degradation. The monsoon climate dominates the Beijing area, characterized by a warm, wet summer and a cold, dry winter with over 70% of annual precipitation falling in May to September (Wang et al., 2005). Thus, it is not surprising for the fast degradation of litters in summer (Fig. 1).

4.2. Effects of litter decomposition on chemical compositions

The chemical compositions of *S. viridis* and *E. indica* showed similar changing patterns with decomposition (Fig. 2). The increase

Table 1
Bulk chemical compositions (mean ± sd) of initial and decomposed grass litters.

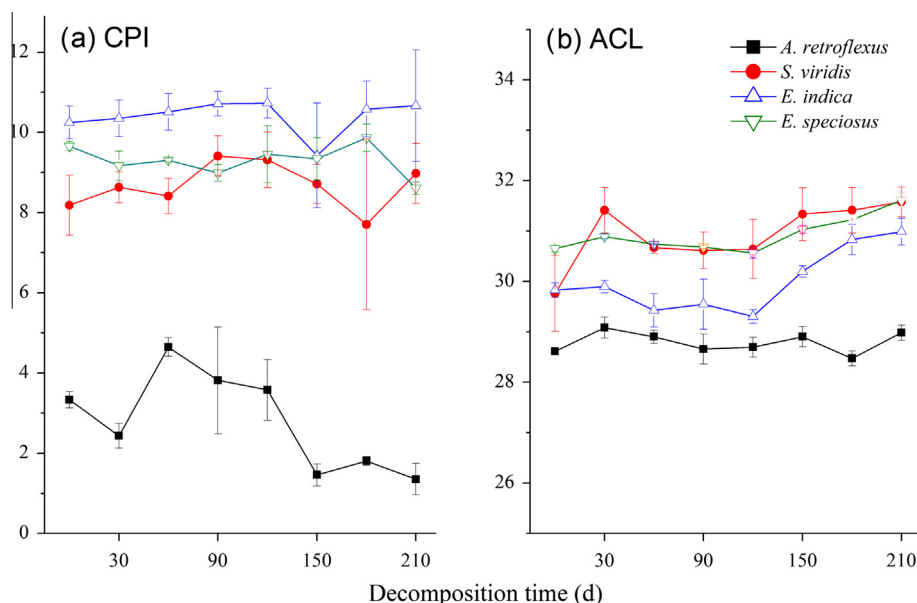| Plants	Decomposition time (day)	C (%)	N (%)	C/N	δ^{13}C (‰)
A. retroflexus	0	43.0 ± 1.9	1.9 ± 0.2	22.4 ± 1.3	−15.3 ± 0.7
	300	39.8	2.3	17.0	−15.3 ± 0.7
S. Viridis	0	37.9 ± 0.3	1.4 ± 0.1	27.6 ± 1.1	−14.5 ± 0.8
	300	38.3	2.3	16.6	−14.8 ± 0.2
E. indica	0	38.9 ± 0.2	1.5 ± 0.1	26.2 ± 2.2	−15.9 ± 0.2
	300	36.2	2.5	14.2	−16.3 ± 0.3
E. speciosus	0	39.1 ± 1.2	3.3 ± 0.1	11.9 ± 0.2	−33.7 ± 0.3
	300	na[a]	na	na	−34.2 ± 0.2

[a] na = Not analyzed.

Fig. 3. Variability in the CPI and ACL values of *n*-alkanes in four grass species in the litterbag experiment.
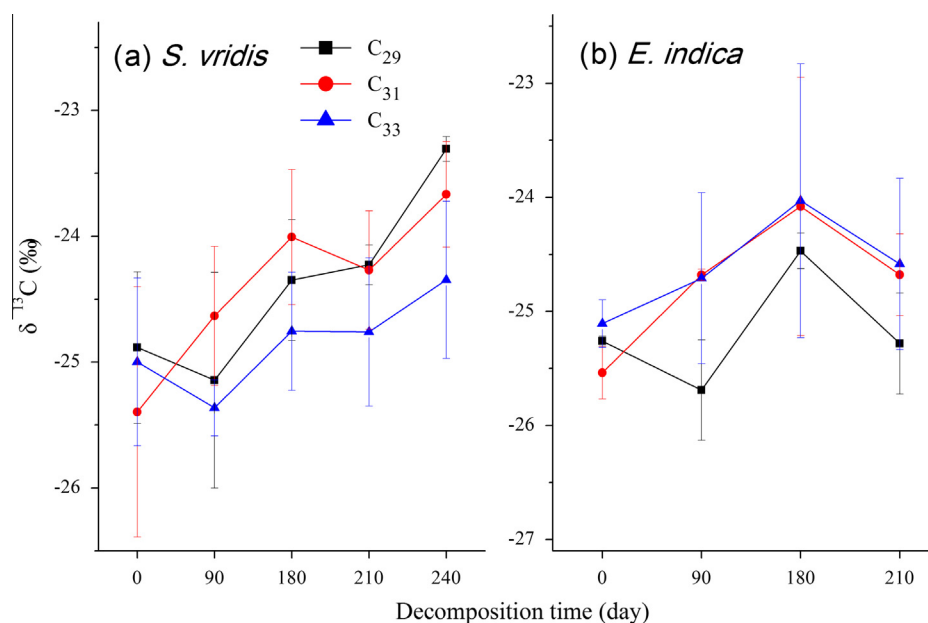

Fig. 4. Variability in the carbon isotope compositions of long chain *n*-alkanes in *S. Viridis* and *E. indica* during the decomposition processes.

of aromatic and aliphatic carbon, the decrease of *O*-alkyl carbon and enhanced alkyl/*O*-alkyl carbon ratio suggest the selected preservation of lignin, tannin, cutin and suberin. This result is consistent with previous findings for diverse plants such as oak, beech and wheat (Preston, 1996; Mathers et al., 2007; Ono et al., 2009). Chemical properties, along with mineral protection and inclusions of organic matter into aggregates or micropores, are the most important mechanisms for the degradation of soil organic matter (Sollins et al., 1996; Dignac et al., 2005; Marschner et al., 2008; Schmidt et al., 2011). Compared to cellulose and carbohydrate, aromatic (e.g., lignin, tannin) and alkyl (e.g., cutin, suberin) compounds are more chemically stable (Kogel-Knabner, 2002; Lorenz et al., 2007), and thus it is not surprising for observed changing patterns in our study. A slightly enhanced proportion of carbonyl carbons is likely due to oxidation of lignin or hydrolysis reactions,

both leading to the formation of carbonyl carbons (Hedges et al., 1988; Ono et al., 2009).

No substantial change of the CPI and ACL in *E. indica*, *S. viridis* and *E. speciosus* in our litterbag experiments suggests that these *n*-alkane proxies are insensitive for early stage litter decomposition, supporting CPI and ACL as robust proxies for the organic matter source. This finding, however, is inconsistent with some results for soil profiles where the CPI and ACL decreased with depth (Huang et al., 1996; Celerier et al., 2009; Buggle et al., 2010). Such disparity cannot be explained by an effect of simple first order kinetic degradation because this "kinetic effect" would only affect the absolute abundance of *n*-alkane homologues but not *n*-alkane ratios (Buggle et al., 2010). It should be pointed out that our study was conducted in a relatively closed litterbag system where short chain *n*-alkanes ($< C_{20}$) were constantly below detection limit,

whereas previous studies investigated in open plant–soil systems (Huang et al., 1996; Celerier et al., 2009; Buggle et al., 2010). Considering this, we attribute different changing patterns of the CPI and ACL to different sources of *n*-alkanes between two systems. Some fungi, bacteria and termites are capable of biosynthesizing a series of *n*-alkanes with different chemical compositions from vascular plants (Weete, 1976; Jurenka and Subchev, 2000; Pedrini et al., 2007). In addition, petroleum also contains a series of *n*-alkanes without apparent OEP (Simoneit and Mazurek, 1982). These non-vascular plant sources may be important contributors for *n*-alkanes in the open soil system but not in the litterbag. Furthermore, vegetation may change in response to natural and anthropogenic impacts (Overpeck et al., 1990; Matthews et al., 2004). Since the abundance and distribution of *n*-alkanes vary among different plants (Maffei, 1996; Schwark et al., 2002; Jansen et al., 2008), overlying vegetation changes can cause shifts in CPI and ACL in soil. Finally, roots as an important contributor to soil organic carbon (Rasse et al., 2005) may have different CPI and ACL compared with aboveground litters. However, root-derived carbon was not investigated in most previous studies of plant decomposition (e.g., Nguyen Tu et al., 2004; Chikaraishi and Naraoka, 2006; Buggle et al., 2010). At the current stage, all these explanations are possible for the decreasing CPI and ACL with depth in soil profiles.

4.3. Carbon isotopic dynamics during early litter decomposition

Our positive $\delta^{13}C$ shift of long chain *n*-alkanes with decomposition agrees with previous studies (Nguyen Tu et al., 2004; Chikaraishi and Naraoka, 2006), but the magnitude of 1.7‰ (Fig. 4) is substantially less than that in the plant–soil systems (up to 12.9‰ with an average of 3–4‰) (Chikaraishi and Naraoka, 2006). A number of factors may explain the carbon isotope change of *n*-alkanes, including different $\delta^{13}C$ values among different plants, seasonal isotopic variations within the same species, external inputs from soil fauna and microbes, kinetic isotopic fractionation and Suess effect (Chikaraishi and Naraoka, 2006). Here we evaluate relative importance of each factor on the observed $\delta^{13}C$ shift.

First, each litterbag in our experiments contains a single grass species collected from the same site and the same season. Thus, the interferences of seasonal isotope variations, different $\delta^{13}C$ among different species, Suess effect and contributions of pre-aged soil organic matter or petroleum derivatives can be excluded, although these effects usually exist in the open plant–soil systems (Chikaraishi et al., 2004; Nguyen Tu et al., 2011). In addition, heterotrophic soil organisms (e.g., termites and bacteria) are potential sources for long chain *n*-alkanes besides vascular plants (Weete, 1976; Matsumoto et al., 1990; Jurenka and Subchev, 2000). Here we estimate the origin of *n*-alkanes based on their distribution patterns since terrigenous vascular plants have much higher CPI and ACL values than other sources (Eglinton and Hamilton, 1967; Meyers, 1997; Jurenka and Subchev, 2000; Buggle et al., 2010). In our study, the CPI and ACL values of *E. indica*, *S. viridis* and *E. speciosus* did not show substantial changes, although 90% of initial litter mass was degraded (Fig. 3). These results strongly suggest that initial litters are a predominant source for long chain *n*-alkanes throughout whole decomposition experiment.

Due to different chemical bond energy between ^{12}C–^{13}C and ^{12}C–^{12}C, a ^{12}C reaction is 4% faster than the corresponding ^{13}C reaction (O'Leary, 1981). Thus, with organic matter degradation, faster chemical reaction rate of ^{12}C than ^{13}C will cause a positive shift of $\delta^{13}C$ of the products, which is one of the kinetic isotopic fractionations (Feng, 2002). A theoretic calculation shows if this fractionation is the sole factor for the $\delta^{13}C$ change, a plot of $\delta^{13}C$ against log (C/C_0) will be a straight line, where C and C_0 are the mass of organic carbon at final and initial time, respectively (Feng,
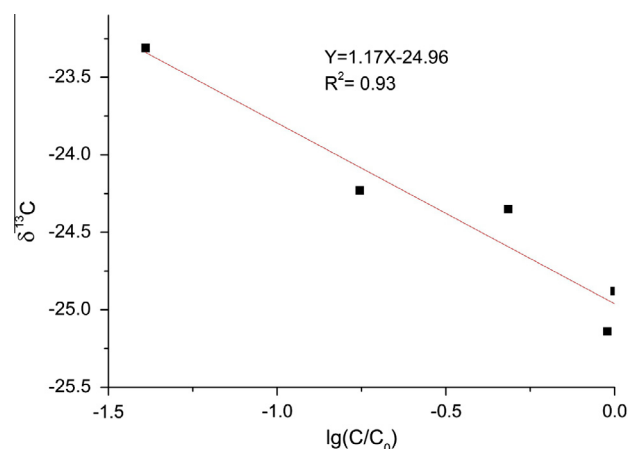
Fig. 5. Correlation between $\delta^{13}C$ and $\log(C/C_0)$ of C_{29} *n*-alkanes in *S. Viridis*, where C and C_0 are the amount of C_{29} *n*-alkanes at the degradation and initial time, respectively.

2002). In our case, a strong linear correlation between $\delta^{13}C$ and $\log(C/C_0)$ of C_{29} *n*-alkane was observed for *S. viridis* ($r^2 = 0.93$; Fig. 5), confirming that the kinetic isotopic fractionation is responsible for observed $\delta^{13}C$ enrichment. However, such strong correlation was not observed for *E. indica*, probably due to limited $\delta^{13}C$ data points (Fig. 4). Nevertheless, our results demonstrated that even though 90% of initial organic matter was degraded, the $\delta^{13}C$ value of long chain *n*-alkanes only varied in a narrow range of 0.6–1.7‰ (Fig. 4). Such magnitude is close to that of bulk soil organic matter during decomposition (1.8–2.8‰) (Wang et al., 2008), but is much less than the $\delta^{13}C$ difference between C_3 and C_4 plants (average of −27‰ versus −13‰) as well as terrigenous C_3 plants and marine phytoplankton (average of −27‰ versus −20‰) (O'Leary, 1981; Farquhar et al., 1989; Meyers, 1997). Therefore, despite the existence of a positive shift with degradation, the carbon isotopic composition of long chain *n*-alkanes, like $\delta^{13}C$ of bulk organic matter, is still valid for tracing organic carbon sources and paleoenvironments. However, in certain environments such as some soils (Chikaraishi and Naraoka, 2006; Nguyen Tu et al., 2011), organisms other than vascular plants such as bacteria, fungi and termites may represent significant sources for *n*-alkanes, thereby amplifying $\delta^{13}C$ alterations.

5. Conclusions

We conducted a 300 d litterbag experiment for four grass species (three C_4 and one C_3 species) to understand chemical and carbon isotopic changes during litter decompositions. Based on solid state ^{13}C NMR, biomarkers and carbon isotopic compositions, several conclusions have been reached. First, with litter degradation, aromatic and alkyl carbon is selectively preserved relative to cellulose and carbohydrates, confirming that chemical property plays an important role in early stage decomposition. Second, > 90% of litter mass loss did not substantially change the *n*-alkane CPI and ACL, warranting these two proxies as robust proxies for organic matter sources and paleoenvironments. Third, with little degradation, a positive shift of the $\delta^{13}C$ of long chain *n*-alkanes is mainly induced by the kinetic isotopic fractionation, but the small magnitude (< 2‰) confirms the applicability of $\delta^{13}C$ of long chain *n*-alkanes in paleoenvironmental studies. Finally, compared to open soil systems, our litterbag experiment presents much less variability in chemical and carbon isotopic compositions. Because additional inputs of *n*-alkanes from soil microbes and fauna can cause changes in both chemical and carbon isotopic compositions, a combined chemical and isotopic approach is strongly recom-

mended for estimation of the carbon source and environmental change. The investigation for different types of plants (trees, shrubs and grasses) and tissues (roots and shoots) are great needed to understand early stage decomposition of organic matter in different ecosystems.

Acknowledgements

*Associate Editor—***Klaas Nierop**

References

Almendros, G., Sanz, J., Velasco, F., 1996. Signatures of lipid assemblages in soils under continental Mediterranean forests. European Journal of Soil Science 47, 183–196.

Baldock, J., Preston, C., McFee, W., Kelly, J., 1995. Chemistry of carbon decomposition processes in forests as revealed by solid-state carbon-13 nuclear magnetic resonance, carbon forms and functions in forest soils. Soil Science Society of America Inc., pp. 89–117.

Bird, M., Pousai, P., 1997. Variations of $\delta^{13}C$ in the surface soil organic carbon pool. Global Biogeochemical Cycles 11, 313–322.

Blagodatskaya, E., Yuyukina, T., Blagodatsky, S., Kuzyakov, Y., 2011. Turnover of soil organic matter and of microbial biomass under C_3–C_4 vegetation change: consideration of ^{13}C fractionation and preferential substrate utilization. Soil Biology & Biochemistry 43, 159–166.

Boutton, T.W., 1996. Stable carbon isotope ratios of soil organic matter and their use as indicators of vegetation and climate change. In: Boutton, T.W., Yamasaki, S. (Eds.), Mass Spectrometry of Soils, pp. 47–82.

Buggle, B., Wiesenberg, G.L.B., Glaser, B., 2010. Is there a possibility to correct fossil *n*-alkane data for postsedimentary alteration effects? Applied Geochemistry 25, 947–957.

Bush, R.T., McInerney, F.A., 2013. Leaf wax *n*-alkane distributions in and across modern plants: Implications for paleoecology and chemotaxonomy. Geochimica et Cosmochimica Acta 117, 161–179.

Celerier, J., Rodier, C., Favetta, P., Lemee, L., Ambles, A., 2009. Depth-related variations in organic matter at the molecular level in a loamy soil: reference data for a long-term experiment devoted to the carbon sequestration research field. European Journal of Soil Science 60, 33–43.

Chikaraishi, Y., Naraoka, H., 2006. Carbon and hydrogen isotope variation of plant biomarkers in a plant–soil system. Chemical Geology 231, 190–202.

Chikaraishi, Y., Naraoka, H., Poulson, S.R., 2004. Carbon and hydrogen isotopic fractionation during lipid biosynthesis in a higher plant (*Cryptomeria japonica*). Phytochemistry 65, 323–330.

Collatz, G.J., Berry, J.A., Clark, J.S., 1998. Effects of climate and atmospheric CO_2 partial pressure on the global distribution of C_4 grasses: present, past, and future. Oecologia 114, 441–454.

Collister, J.W., Rieley, G., Stern, B., Eglinton, G., Fry, B., 1994. Compound specific $\delta^{13}C$ analyses of leaf lipids from plants with differing carbon dioxide metabolisms. Organic Geochemistry 21, 619–627.

Cortez, J., 1998. Field decomposition of leaf litters: relationships between decomposition rates and soil moisture, soil temperature and earthworm activity. Soil Biology & Biochemistry 30, 783–793.

Deines, P., 1980. The Isotopic Composition of Reduced Organic Carbon. Elsevier, Amsterdam.

Diefendorf, A.F., Mueller, K.E., Wing, S.L., Koch, P.L., Freeman, K.H., 2010. Global patterns in leaf ^{13}C discrimination and implications for studies of past and future climate. Proceedings of the National Academy of Sciences 107, 5738–5743.

Dignac, M.F., Bahri, H., Rumpel, C., Rasse, D.P., Bardoux, G., Balesdent, J., Girardin, C., Chenu, C., Mariotti, A., 2005. Carbon-13 natural abundance as a tool to study the dynamics of lignin monomers in soil: an appraisal at the Closeaux experimental field (France). Geoderma 128, 3–17.

Eglinton, G., Hamilton, R.J., 1967. Leaf epicuticular waxes. Science 156, 1322–1335.

Ehleringer, J.R., Sage, R.F., Flanagan, L.B., Pearcy, R.W., 1991. Climate change and the evolution of C_4 photosynthesis. Trends in Ecology & Evolution 6, 95–99.

Farquhar, G.D., Ehleringer, J.R., Hubick, K.T., 1989. Carbon isotope discrimination and photosynthesis. Annual Review of Plant Biology 40, 503–537.

Feng, X., 2002. A theoretical analysis of carbon isotope evolution of decomposing plant litters and soil organic matter. Global Biogeochemical Cycles 16, 1119.

Hayes, J., Freeman, K.H., Popp, B.N., Hoham, C.H., 1990. Compound-specific isotopic analyses: a novel tool for reconstruction of ancient biogeochemical processes. Organic Geochemistry 16, 1115–1128.

Hedges, J.I., Blanchette, R.A., Weliky, K., Devol, A.H., 1988. Effects of fungal degradation on the CuO oxidation products of lignin: a controlled laboratory study. Geochimica et Cosmochimica Acta 52, 2717–2726.

Hu, K., Li, B., Lü, Y., Duan, Z., Li, Z., Li, G., Sun, D., 2006. Spatial variation of physico-chemical properties in Shangzhuang experimental station of China Agricultural University. Journal of China Agricultural University 11, 27–33 (in Chinese).

Huang, Y., Bol, R., Harkness, D.D., Ineson, P., Eglinton, G., 1996. Post-glacial variations in distributions, ^{13}C and ^{14}C contents of aliphatic hydrocarbons and bulk organic matter in three types of British acid upland soils. Organic Geochemistry 24, 273–287.

Huang, Y., Eglinton, G., Ineson, P., Latter, P.M., Bol, R., Harkness, D.D., 1997. Absence of carbon isotope fractionation of individual *n*-alkanes in a 23-year field decomposition experiment with *Calluna vulgaris*. Organic Geochemistry 26, 497–501.

Huang, X., Xue, J., Zhang, J., Qin, Y., Meyers, P.A., Wang, H., 2012. Effect of different wetness conditions on Sphagnum lipid composition in the Erxianyan peatland, central China. Organic Geochemistry 44, 1–7.

Jansen, B., Nierop, K.G.J., 2009. Methyl ketones in high altitude Ecuadorian Andosols confirm excellent conservation of plant-specific *n*-alkane patterns. Organic Geochemistry 40, 61–69.

Jansen, B., Haussmann, N.S., Tonneijck, F.H., Verstraten, J.M., de Voogt, P., 2008. Characteristic straight-chain lipid ratios as a quick method to assess past forest–páramo transitions in the Ecuadorian Andes. Palaeogeography, Palaeoclimatology, Palaeoecology 262, 129–139.

Jurenka, R.A., Subchev, M., 2000. Identification of cuticular hydrocarbons and the alkene precursor to the pheromone in hemolymph of the female gypsy moth, *Lymantria dispar*. Archives of Insect Biochemistry and Physiology 43, 108–115.

Kögel-Knabner, I., 1997. ^{13}C and ^{15}N NMR spectroscopy as a tool in soil organic matter studies. Geoderma 80, 243–270.

Kogel-Knabner, I., 2002. The macromolecular organic composition of plant and microbial residues as inputs to soil organic matter. Soil Biology & Biochemistry 34, 139–162.

Kohn, M.J., 2010. Carbon isotope compositions of terrestrial C_3 plants as indicators of (paleo) ecology and (paleo) climate. Proceedings of the National Academy of Sciences 107, 19691–19695.

Li, R.-H., Deng, Q., Zhou, g., Zhang, D., 2011. Effect of incubation starting time on litter decomposition rate in a subtropical forest in China. Chinese Journal of Plant Ecology 35, 699–706.

Lorenz, K., Lal, R., Preston, C.M., Nierop, K.G.J., 2007. Strengthening the soil organic carbon pool by increasing contributions from recalcitrant aliphatic bio(macro)molecules. Geoderma 142, 1–10.

Maffei, M., 1996. Chemotaxonomic significance of leaf wax alkanes in the Gramineae. Biochemical Systematics and Ecology 24, 53–64.

Marschner, B., Brodowski, S., Dreves, A., Gleixner, G., Gude, A., Grootes, P.M., Hamer, U., Heim, A., Jandl, G., Ji, R., Kaiser, K., Kalbitz, K., Kramer, C., Leinweber, P., Rethemeyer, J., Schäffer, A., Schmidt, M.W.I., Schwark, L., Wiesenberg, G.L.B., 2008. How relevant is recalcitrance for the stabilization of organic matter in soils? Journal of Plant Nutrition and Soil Science 171, 91–110.

Marseille, F., Disnar, J.R., Guillet, B., Noack, Y., 1999. *N*-Alkanes and free fatty acids in humus and A1 horizons of soils under beech, spruce and grass in the Massif-Central (Mont-Lozère), France. European Journal of Soil Science 50, 433–441.

Mathers, N.J., Jalota, R.K., Dalal, R.C., Boyd, S.E., 2007. ^{13}C-NMR analysis of decomposing litter and fine roots in the semi-arid Mulga Lands of southern Queensland. Soil Biology & Biochemistry 39, 993–1006.

Matsumoto, G.I., Akiyama, M., Watanuki, K., Torii, T., 1990. Unusual distributions of long-chain *n*-alkanes and *n*-alkenes in Antarctic soil. Organic Geochemistry 15, 403–412.

Matthews, H., Weaver, A., Meissner, K., Gillett, N., Eby, M., 2004. Natural and anthropogenic climate change: incorporating historical land cover change, vegetation dynamics and the global carbon cycle. Climate Dynamics 22, 461–479.

Melillo, J.M., Aber, J.D., Linkins, A.E., Ricca, A., Fry, B., Nadelhoffer, K.J., 1989. Carbon and nitrogen dynamics along the decay continuum: plant litter to soil organic matter. In: Ecology of Arable Land-Perspectives and Challenges. Springer, pp. 53–62.

Meyers, P.A., 1997. Organic geochemical proxies of paleoceanographic, paleolimnologic, and paleoclimatic processes. Organic Geochemistry 27, 213–250.

Murphy, K.L., Klopatek, J.M., Klopatek, C.C., 1998. The effects of litter quality and climate on decomposition along an elevational gradient. Ecological Applications 8, 1061–1071.

Nguyen Tu, T.T., Derenne, S., Largeau, C., Bardoux, G., Mariotti, A., 2004. Diagenesis effects on specific carbon isotope composition of plant *n*-alkanes. Organic Geochemistry 35, 317–329.

Nguyen Tu, T.T., Egasse, C., Zeller, B., Bardoux, G., Biron, P., Ponge, J.-F., David, B., Derenne, S., 2011. Early degradation of plant alkanes in soils: a litterbag experiment using ^{13}C-labelled leaves. Soil Biology & Biochemistry 43, 2222–2228.

O'Leary, M.H., 1981. Carbon isotope fractionation in plants. Phytochemistry 20, 553–567.

Ono, K., Hirai, K., Morita, S., Ohse, K., Hiradate, S., 2009. Organic carbon accumulation processes on a forest floor during an early humification stage in a temperate deciduous forest in Japan: evaluations of chemical compositional changes by ^{13}C NMR and their decomposition rates from litterbag experiment. Geoderma 151, 351–356.

Overpeck, J.T., Rind, D., Goldberg, R., 1990. Climate-induced changes in forest disturbance and vegetation. Nature 343, 51–53.

Pedrini, N., Crespo, R., Juárez, M.P., 2007. Biochemistry of insect epicuticle degradation by entomopathogenic fungi. Comparative Biochemistry and Physiology Part C: Toxicology & Pharmacology 146, 124–137.

Prescott, C., Zabek, L., Staley, C., Kabzems, R., 2000. Decomposition of broadleaf and needle litter in forests of British Columbia: influences of litter type, forest type, and litter mixtures. Canadian Journal of Forest Research 30, 1742–1750.

Preston, C.M., 1996. Applications of NMR to soil organic matter analysis: history and prospects. Soil Science 161, 144–166.

Rasse, D.P., Rumpel, C., Dignac, M.F., 2005. Is soil carbon mostly root carbon? Mechanisms for a specific stabilisation. Plant and Soil 269, 341–356.

Rieley, G., Collister, J.W., Stern, B., Eglinton, G., 1993. Gas chromatography/isotope ratio mass spectrometry of leaf wax *n*-alkalines from plants of differing carbon dioxide metabolisms. Rapid Communications in Mass Spectrometry 7, 488–491.

Schmidt, M.W., Torn, M.S., Abiven, S., Dittmar, T., Guggenberger, G., Janssens, I.A., Kleber, M., Kögel-Knabner, I., Lehmann, J., Manning, D.A., 2011. Persistence of soil organic matter as an ecosystem property. Nature 478, 49–56.

Schwark, L., Zink, K., Lechterbeck, J., 2002. Reconstruction of postglacial to early Holocene vegetation history in terrestrial central Europe via cuticular lipid biomarkers and pollen records from lake sediments. Geology 30, 463–466.

Simoneit, B.R., Mazurek, M.A., 1982. Organic matter of the troposphere—II. Natural background of biogenic lipid matter in aerosols over the rural western United States. Atmospheric Environment 16, 2139–2159.

Sollins, P., Homann, P., Caldwell, B.A., 1996. Stabilization and destabilization of soil organic matter: mechanisms and controls. Geoderma 74, 65–105.

Vandenbroucke, T.R.A., Munnecke, A., Leng, M.J., Bickert, T., Hints, O., Gelsthorpe, D., Maier, G., Servais, T., 2013. Reconstructing the environmental conditions around the Silurian Ireviken Event using the carbon isotope composition of bulk and palynomorph organic matter. Geochemistry, Geophysics, Geosystems 14, 86–101.

Wang, P., Clemens, S., Beaufort, L., Braconnot, P., Ganssen, G., Jian, Z., Kershaw, P., Sarnthein, M., 2005. Evolution and variability of the Asian monsoon system: state of the art and outstanding issues. Quaternary Science Reviews 24, 595–629.

Wang, G., Feng, X., Han, J., Zhou, L., Tan, W., Su, F., 2008. Paleovegetation reconstruction using $\delta^{13}C$ of soil organic matter. Biogeosciences 5, 1325–1337.

Wang, G., Li, J., Liu, X., Li, X., 2013a. Variations in carbon isotope ratios of plants across a temperature gradient along the 400 mm isoline of mean annual precipitation in north China and their relevance to paleovegetation reconstruction. Quaternary Science Reviews 63, 83–90.

Wang, W., Zhang, X., Tao, N., Ao, D., Zeng, W., Qian, Y., Zeng, H., 2013b. Effects of litter types, microsite and root diameters on litter decomposition in *Pinus sylvestris* plantations of northern China. Plant and Soil 374, 677–688.

Wedin, D.A., Tieszen, L.L., Dewey, B., Pastor, J., 1995. Carbon isotope dynamics during grass decomposition and soil organic matter formation. Ecology, 1383–1392.

Weete, J.D., 1976. Algal and fungal waxes. In: Kolattukudy, P.E. (Ed.), Chemistry and Biochemistry of Natural Waxes. Elsevier, New York, pp. 49–418.

Wider, R.K., Lang, G.E., 1982. A critique of the analytical methods used in examining decomposition data obtained from litter bags. Ecology, 1636–1642.

Zhang, Z., Zhao, M., Eglinton, G., Lu, H., Huang, C.-Y., 2006. Leaf wax lipids as paleovegetational and paleoenvironmental proxies for the Chinese Loess Plateau over the last 170 kyr. Quaternary Science Reviews 25, 575–594.